The use of magnetic nanoparticles in hyperthermia of Ehrlich tumor

Sahar E. Abo-Neima, Hussein A. Motaweh, and Rahma M.Anany

Department of physics, Faculty of Science, Damanhur University, Egypt.
Sahar_amr2002@yahoo.com

Abstract: Hyperthermia has been in use for many years, as a potential alternative method in cancer treatment, and high frequency microwave radiation has been used successfully to raise the tumor temperature to around 42°C in superficial tumors without causing damage to surrounding healthy tissues. In the present work a total of 60 male mice weighing 20-25gm of 4-5 weeks of age will be used in all the experiments. A suspension of 10^6 cells/ mL isolated from Ehrlich ascites carcinoma in mice will be prepared. The animals will be injected into the left flank with 0.2mL of this suspension. When tumors reach approximately 5-10 mm in diameter, mice will be randomly divided into nine groups, each of ten namely from G_1 to G_9:1st group which injected with phosphate buffer (control group). 2nd group which mice bearing tumor without injection with magnetic nanoparticles (MNPs) and without hyperthermia (Tumor).3rd group which mice bearing tumor exposed to microwave hyperthermia without injection of MNPs (MW). 4th group which mice bearing tumor injected with ferric MNPs (FE) without hyperthermia.5th group which mice bearing tumor injected with ferric MNPs and exposed to microwave hyperthermia (FE+MW).6th group which mice bearing tumor injected with Nickel MNPs without hyperthermia (NI).7th group which mice bearing tumor injected with MNPs and exposed to microwave hyperthermia (NI+MM).8[th]group which mice bearing tumor injected with MNPs without hyperthermia (CO).9th group which mice bearing tumor injected with cobalt MNPs and exposed to microwave hyperthermia (CO+MW). The results showed that The transmission electron microscope (TEM) image shows that the prepared magnetite nanoparticles are almost spherical shape. The particles have tendency to aggregate because of their magnetic properties. The average particle size as determine from the histogram is ~ 20 nm for Fe and 100nm for Co and Ni. The electron diffraction shows that the sample are completely crystalline as confirmed from the x-ray diffraction (XRD) and there was highly significant decreased in the normalized tumor size with the different treatment modalities as compared with the animal bearing tumor (control group). The very high significant decreased for Ni+MW treatment was indicated i. e. the treatment of ehrlich tumor with Ni+MW give us the most inhibition for tumor size. From the histopathological study for ehlich tumor where tumors were treated with MNPs and with NPs +MW which exhibits tumor necrosis and fibrosis. It was concluded that MNPs can penetrate tumor tissue and pass through gaps, are able to remain in the tumor tissue and destroyed cancer cells.

Keywords: Ehlich tumor, microwave, nanoparticles, TEM, XRD, histopathology

1. Introduction

Hyperthermia, also often called thermal therapy or thermotherapy, is a cancer treatment in which cancer tissue or the whole body is exposed to temperatures between 41-43°C through the application of electromagnetic energy for a defined period of time to damage and kill cancer cells. Above this temperature, heat has a direct cytotoxic effect on both normal and tumor cells and is referred to as thermal ablation. Hyperthermia causes changes in tissue physiology. An increase in temperature due to hyperthermia changes the microcirculation of the tumor and hence the oxygenation (Franckena & van der Zee., 2010)[1]. The effects of hyperthermia on cancer can significantly disrupt a tumor cell's capacity to divide, leading to shrinkage of tumors (Nikfarjam et al., 2005)[2]. Radiative hyperthermia for heat generation uses the lower frequency waves such as microwave (MW). MW hyperthermia has generally utilized single waveguide microwave antennas. A widely used method for electromagnetic energy delivery is antenna-array coupling. The body is ringed by the antenna array which delivers chosen field intensity with controlled phase and frequency. The major problem of applied hyperthermia treatments is achieving a homogenous heat distribution in the treated tissue (Habash et al., 2006)[3]. The currently available modalities of hyperthermia are often limited by their inability to selectively target tumor tissue and, hence, they carry a risk of collateral organ damage or they deposit heat in a localized manner, which can result in under-treatment of a tumor. Nanotechnology-based cancer therapy is a special form of interstitial thermotherapy with the advantage of selective heat deposition to the tumor cells. This new therapy is one

of the first applications of nanotechnology in medicine and is based on heating of nanoparticles.

Microwave hyperthermia is a non-ionizing form of radiation therapy that can substantially improve results for cancer treatment. Tumors cells are considered to be more susceptible to hyperthermia effects than healthy cells because of higher metabolic rate. Hyperthermia has been proven to increase the response of malignant tumors to radiation therapy in both experimental animal tumors and the clinical treatment of human cancer. This treatment is toxic for the tumor itself, making the tumor more sensitive to traditional chemo- and radiation therapies. This in turn leads to reducing treatment side effects by reducing radiation doses and cytostatic drugs with unchanged treatment results (Rasha et al.,2013)[4].

Nanoparticles NPs are submicron moieties (between 1nm and 100nm according to the usual definition, although there are examples of NPs several hundreds of nanometers in size) made of inorganic or organic (e.g. polymeric) materials, which may or may not be biodegradable. Their importance relates to the fact that the characteristics of NPs are different from those of bulk materials of the same composition, which is mainly because of size effects, the magnetic and electronic properties, and the role played by surface phenomena as the size is reduced (Manuel Arruebo et al., 2007)[5].

The idea of using nanoparticle hyperthermia to treat tumors. This method involved the injection of magnetic nanoparticles directly tumors and exciting these nanoparticles with microwave to produce heat and reduced tumor size.
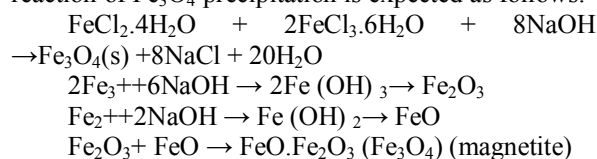
The purpose of this study is to compare the temperature distribution and tissue necrosis pattern after hyperthermia treatment of Ehrlich tumor in the presence and absence of magnetic nanoparticles using microwave heating devices.

2. Material and Methods
2.1: Preparation and Characterization of Magnetic nanoparticles:
2.1.1: Preparation of magnetic nanoparticle

Magnetic nanoparticles (Fe_3O_4) were prepared using co-precipitation method with a ferrous complex in presence of NaOH. The 1:2 molar ratio of ferrous to ferric chloride (Fe^{2+}/Fe^{3+}), in the presence of aqueous sodium hydroxide have formed the magnetites (An-Hui et al.,2007)[6]. The chemical reaction of Fe_3O_4 precipitation is expected as follows:

$FeCl_2.4H_2O$ + $2FeCl_3.6H_2O$ + $8NaOH$ $\rightarrow Fe_3O_4(s)$ $+8NaCl + 20H_2O$

$2Fe_3++6NaOH \rightarrow 2Fe\,(OH)_3 \rightarrow Fe_2O_3$

$Fe_2++2NaOH \rightarrow Fe\,(OH)_2 \rightarrow FeO$

$Fe_2O_3+ FeO \rightarrow FeO.Fe_2O_3\ (Fe_3O_4)$ (magnetite)

But cobalt and nickel nanoparticles were obtained from Sigma Aldrich with its characterization.
2.1.2. Characterization of magnetic nanoparticles

The prepared magnetite nanoparticles have been explained in the experimental part and characterized via Transmission electron microscopy (TEM), X-ray Diffraction (XRD) and vibrating sample magnatometer (VSM).
2.1.2.1. Transmission electron microscopy (TEM)

Physical size and shape of the prepared iron oxide particles were determined by TEM (JEOL-100 CX). For this purpose, a drop of this magnetic nanoparticles (MNPs) solution was loaded onto a 400-mesh carbon-coated copper grid and the solvent was allowed to evaporate in the air, and then screened under TEM.
2.1.2.2. X-ray Diffraction (XRD analysis)

The dried MNPs were analyzed for the crystalline nature of MNPs by X-ray diffractometer (Shimaduz, XRD- 7000, Maxima, and Japan). The crystallite domain size was calculated from the width of the XRD peaks, assuming that they are free from non-uniform strains, using the Scherer's equation as follow:

$D = 0.94\ \lambda/\beta Cos\ \theta$ **(1)**

Where D is the average crystallite domain size perpendicular to the reflecting planes, λ is the X-ray wavelength, β is the full width at half maximum (FWHM), and θ is the diffraction angle. This modified formula is valid only when the crystallite size is smaller than 100 nm (Pushpa et al., 2013)[7].
2.1.2.3. Particle size analyzer

The particle size distribution of the MNPs was determined by laser light scattering using a Beckman Coulter Particle Size Analyzer (N5 submicron particle size analyzer, Japan). Magnetic fluid was added to the sample dispersion unit containing the stirrer and stirred to reduce the aggregation, and the laser obscuration range was maintained at 15-20%. The mean particle size was measured after performing the experiment in triplicates.
2.2. Experimental Animals:

In the present work a total of 60 male mice weighing 20-25gm of 4-5 weeks of age will be used in all the experiments. A suspension of 10^6 cells/mL isolated from Ehrlich ascites carcinoma in mice will be prepared. The animals will be injected into the left flank with 0.2mL of this suspension. When tumors reach approximately 5-10mm in diameter, mice will be randomly divided into the following groups, each of ten mice as follows:

G_1: mice injected with phosphate buffer (control).

G_2: mice bearing tumor without injection with MNPs and without hyperthermia (Tumor).

G₃: mice bearing tumor exposed to microwave hyperthermia without injection of MNPs (MW). **G₄**: mice bearing tumor injected with magnetic nanoparticles without hyperthermia (FE).

G₅: mice bearing tumor injected with magnetic nanoparticles and exposed to microwave hyperthermia (FE+MW).

G₆: mice bearing tumor injected with MNPs without hyperthermia (NI).

G₇: mice bearing tumor injected with MNPs and exposed to microwave hyperthermia (NI+MM).

G₈: mice bearing tumor injected with MNPs without hyperthermia (CO).

G₉: mice bearing tumor injected with magnetic nanoparticles and exposed to microwave hyperthermia (CO+MW).

2.3. Exposure facility system
2.3.1. Microwave Generator

Fig.1. indicates the block diagram of microwave system unit. The heart of the microwave generator is the magnetron. This device is basically a vacuum tube operated in a magnetic field to produce microwave energy directly. The magnetron filament was heated with the use of dc current to improve the stability of the filament temperature. High voltage potential difference was applied between the cathode and the anode of the magnetron. The magnetron output power is directly related to the dc of the high voltage power supply. This microwave generator produces a microwave of maximum continuous power 100W at a frequency of 2450 MHz (Mohammed et al., 1989)[8]. Hyperthermia is currently being used as an adjunct to radiation therapy and chemotherapy of superficial malignancies. However, use of hyperthermia is limited despite reported efficacy in both laboratory and clinical application. This phenomenon is due primarily to lack of efficient heating applicators capable of heating large volume (or area) tumors that typically require adjuvant therapy up to therapeutic temperatures. In addition, the lack of reliable temperature feedback control systems which can be implemented noninvasively limits the options of clinicians during treatment (Masunaga et al., 1990 & Anderson et al., 1990 & Kapp et al., 1992)[9, 10, 11].
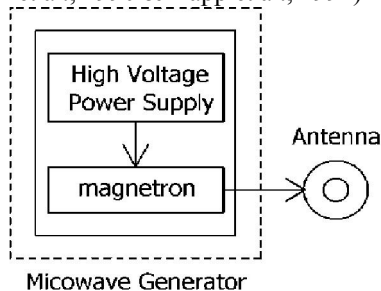

Figure 1. Block diagram of MW system unit.

2.4. Tumor size measurements

Due to the high growth rate in Ehrlich tumor model, change in tumor volume (Vmm^3) was monitored over a 14day period for treated and control group. Ellipsoidal tumor volume was assessed every day and tumor volume (V) was calculated using the formula

$$V = (\pi/6) \, (d)2 \, (D) \quad (2)$$

Where **D** and **d** are the long and short axes respectively. Tumor diameters were measured with digital Vernier calipers. Mice were selected for treatment when the tumors reached the desired volume ($0.7–1cm^3$). Multivariate analysis of variance (MANOVA) was carried out to investigate the effect of both time (from day 0 up to day 15) and type of treatment on tumor growth. T-TEST (least significance difference) multiple-comparison test was also conducted to check the significance between group pairs.

2.5. Biochemical parameter

For the biochemical tests, about 2–3mL of blood sample depending on the rat weight was collected into a centrifuge tube without any anticoagulant. The centrifuge tube was left for about 15min to allow blood coagulation. Clear serum samples were then separated by centrifugation at 1000g for 20 min. Serum samples were separated in glass tubes, labeled and stored in deep freezer at -50°C for different biochemical analysis for different biochemical assays. However, determination of enzyme activities was carried out on fresh serum samples. Serum aspartate amino transferase (AST) is an enzyme belonging to the class of transferases. AST activity is measured by using optimized ultraviolet-test according to International Federation of Clinical Chemistry and Laboratory Medicine (IFCC) (Thomas. 1998)[12]. Serum alanine aminotransferase (ALT) is a transferase with enzymeatic activity similar to AST (Moss & Henderson.,1999)[13].

3.6. Histopathological investigation

Sections were taken from liver immediately after killing the rats. These samples were fixed in 10% buffered neutral formalin solution. Then after proper fixation, the samples were dehydrated in ascending grades of ethyl alcohol (50-100%), then cleared in xylol, embedded in paraffin and finely blocking occurred. These samples were sectioned at 5μm in thickness and stained with hematoxylin and eosin (H & E) for microscopical examination (Rabab et al., 2014)[14].

2.7. Statistical Analysis of Data:

The data were analyzed using one-way analysis of variance (ANOVA). Results were expressed as mean ± standard error (SE) and values of P>0.05 were considered non-significantly different, while those of P < 0.05 and P < 0.01 were considered significant and

highly significant, respectively. F probability expresses the general effect between groups.

3. Results & Discussion

In this dissertation a study of enhanced hyperthermia for cancer treatment through the use of magnetic nanoparticles is presented. Hyperthermia has been in use for many years, as a potential alternative method in cancer treatment, and high frequency microwave radiation has been used successfully to raise the tumor temperature to around 42°C in superficial tumors without causing damage to surrounding healthy tissues. Magnetic fluid hyperthermia involves the use of magnetic nanoparticles injected into the tumor before exposure to microwave radiation. The magnetic energy in the nanoparticles is converted into heat allowing for amore maintain of temperature in the tumor to the desired level. Hyperthermia is one of the most promising new multidisciplinary approaches to cancer therapy. Cancer cells exhibit both lower electrical membrane potentials and lower electrical impedance than normal cells. Since injured and cancerous cells cannot maintain a normal membrane potential they will have electronic dysfunctions that will impede repair and the reestablishment of normal metabolic functions. Therefore a key component of cell repair and cancer treatment would be to reestablish a healthy membrane potential in the body's cells (Rasha et al., 2013)[4].
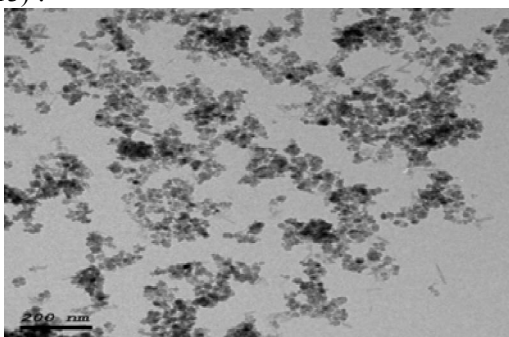

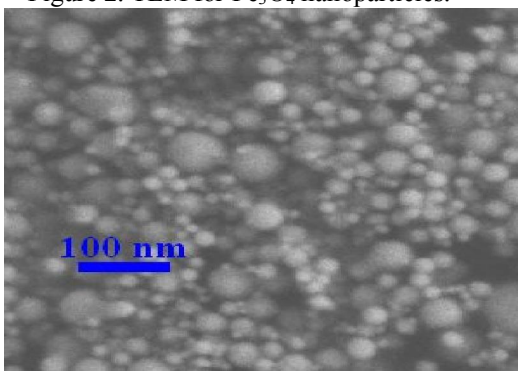Figure 2. TEM for Fe$_3$O$_4$ nanoparticles.
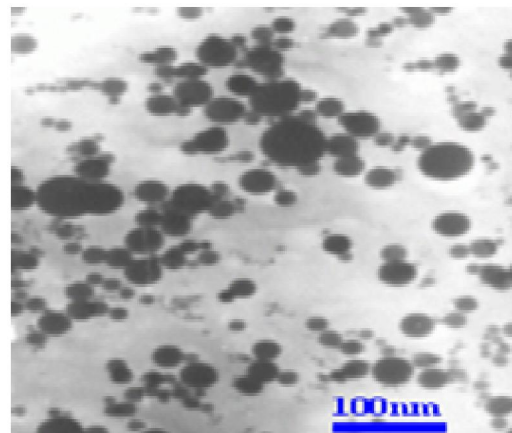

Figure 3. TEM for Co nanoparticles.

Figure 4. TEM for Ni nanoparticles

Iron oxide, Nickel and Cobalt nanoparticles were considered for this study as they are non-toxic and bio-compatible. Various characteristics of the nanoparticles such as radius, magnetic susceptibility and concentration were considered. The physical size and shape of the nanoparticles were determined by TEM. (Fig.2, 3 and 4) shows TEM for the magnetite nanoparticles are almost spherical shape. The particles have tendency to aggregate because of their magnetic properties. The average particle size as determine from the histogram is ~ 200 nm for Fe$_3$O$_4$. The TEM for Ni and Co nanoparticles which revealed the average particle size as determine from both histogram is ~ 100 nm (Fig.3 & 4) respectively.
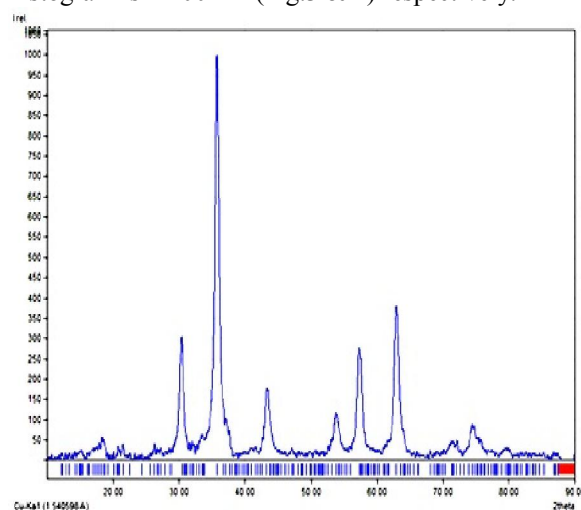

Figure 5. XRD pattern of Fe$_3$O$_4$ nanoparticles

The electron differaction shows that the sample are completely crystalline as confirmed from the XRD (Fig.5,6 and7). XRD data of the NPs samples of the prepared Fe$_3$O$_4$ nanoparticles which confirms the formation of the required cubic ferrite without other unwanted phases in fair consistency with the standard card shown below and with XRD patterns. The

reflection peaks represents the (220), (311), (400), (422), (511), and (440) planes characteristic of Fe_3O_4 (Fig.5).
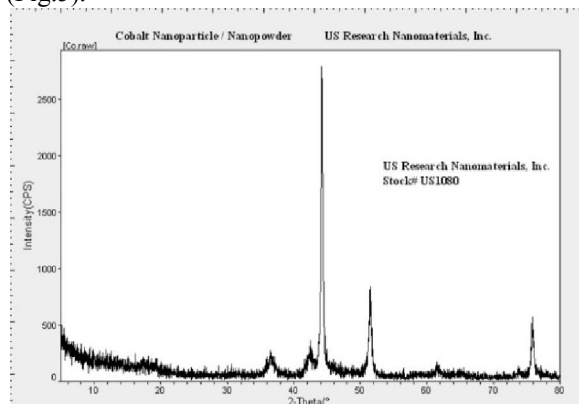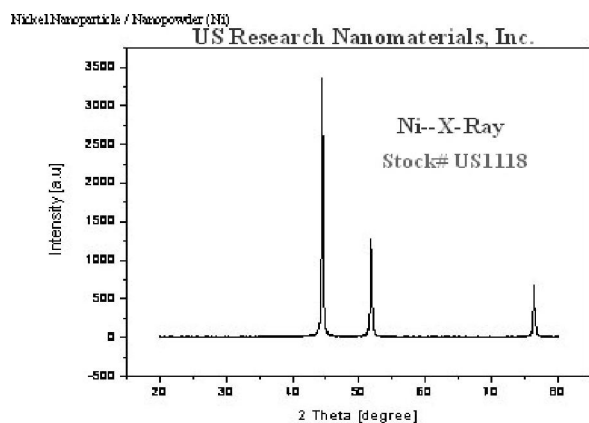

Figure 6. XRD pattern of Co nanoparticles

Figure 7. XRD pattern of Ni nanoparticles

Relative tumor size variation data obtained for each group at the end of the treatment period, 14 days, are analyzed statistically, the results obtained are indicated in Fig.8. It is clear from this figure that there was highly significant decreased in the normalized tumor size with the different treatment modalities as compared with the animal bearing tumor (control group). The very high significant decreased for Ni+MW treatment was indicated i.e. the treatment of ehrlich tumor with Ni+MW give us the most inhibition for tumor. Data presented in Table.1. revealed that Serum Aspartate transferase (AST) activity showed a very highly significant decreased in (MW and Fe) groups as compared to tumor group. Moreover, a non-significant decrease in (AST) activity as compared to (Tumor) group for the remained experimental group. Serum Alanine transferase (ALT) activity revealed to a very high significant decreased in serum (ALT) activities for MW group and extremely significant changes in ALT activity for Fe+ MW group but non-significant

changes in (AST) activity as compared to (Tumor) group for the remained experimental group. Serum creatinine concentration showed very highly significant decreased in MW followed by extremely significant increase in Co group as compared to (Tumor) group. Serum Urea concentration showed a significant decrease in MW and Fe+MW groups followed by a non-significant changes for other groups. From this results we concluded that the treatment of ehrlich tumor with Ni, Co, Ni+MW and Co+MW not exhibit any side effects on liver enzyme and kidney function except for Ni only decreased urea concentrations.
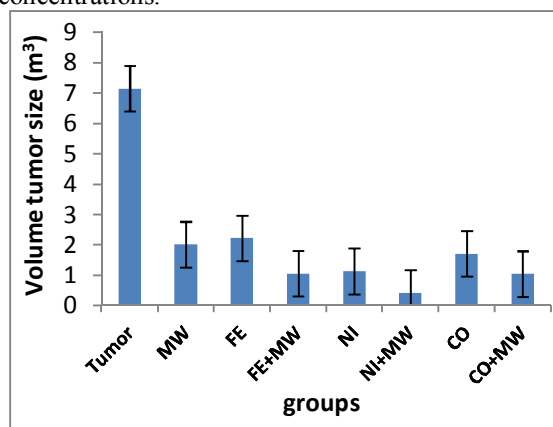

Figure 8. indicates volume tumor size for all groups as compared with the animal bearing tumor (control group).

Nanoparticles can also easily permeate tumor vasculature and remain in tumors, as gaps in tumor vasculature in the range of 100nm to 2μm, and are larger than the gaps in the endothelial lining of normal (healthy) capillaries. Nanoparticles easily pass through these gaps, and because tumors lack lymphatic clearance and have a disordered extracellular matrix, are able to remain in the tumor *tissue* (Jihyoun et al., 2014)[15]. Nanoparticles may bind to a receptor and cause some cellular/tissue responses (e.g., change in the electrical activity of the cell), blocking the growth and spread of disease by interfering with cancer cells involved in tumor growth and progression. The recorded decreased in plasma ALT and AST activities in tumor bearing mice of the present study might be due to generalized destruction of liver cells and release of AST into plasma after tumor induction. On the other hand, a significant decreased in serum urea concentration. The decreased in urea production as a result of catabolic effect of tumor. Our results demonstrated a very highly significant change in serum creatinine concentration in tumor bearing mice. serum creatinine level showed a significant decreased in mice-bearing Ehrlich ascites carcinoma due to muscle necrosis.

Table 1. Effect NPs on AST, ALT, Urea and creatinine in plasma.

| Groups /parameters	Liver function		Kidney function	
	AST (U/ l)	ALT (U/ l)	Urea mmol / l	Creatinine mg/dl
Tumor	165.86±30.71	1147.86±119.20	30.61±1.6	0.37±0.04
NC	146.57±5.86	643.57±45.46	45.86±1.58	7.77±7.21
MW	21.41±0.18^{VHS}	92.29±0.95^{VHS}	6.97±0.06^{ES}	0.14±0.02^{ES}
FE	36.24±0.26^{VHS}	1098.63±0.79^{NS}	7.76±0.16^{ES}	0.34±0.32^{NS}
FE+MW	159.87±0.34^{NS}	122.36±4.65^{ES}	5.93±0.08^{ES}	0.25±0.02^{SS}
NI	204.29±31.92^{NS}	1036.86±172.94^{NS}	23.7±1.27^{VS}	0.3±0.01^{NS}
NI+MW	152.71±6.26^{NS}	1222.29±81.22^{NS}	39.14±3.94^{NS}	0.31±0.01^{NS}
Co	139.71±3.43^{NS}	1935.71±113.41^{ES}	30.56±0.73^{NS}	0.33±0.01^{NS}
Co+MW	173±2.83^{NS}	1139.86±8.91^{NS}	29.94±0.25^{NS}	0.3±0.01^{NS}
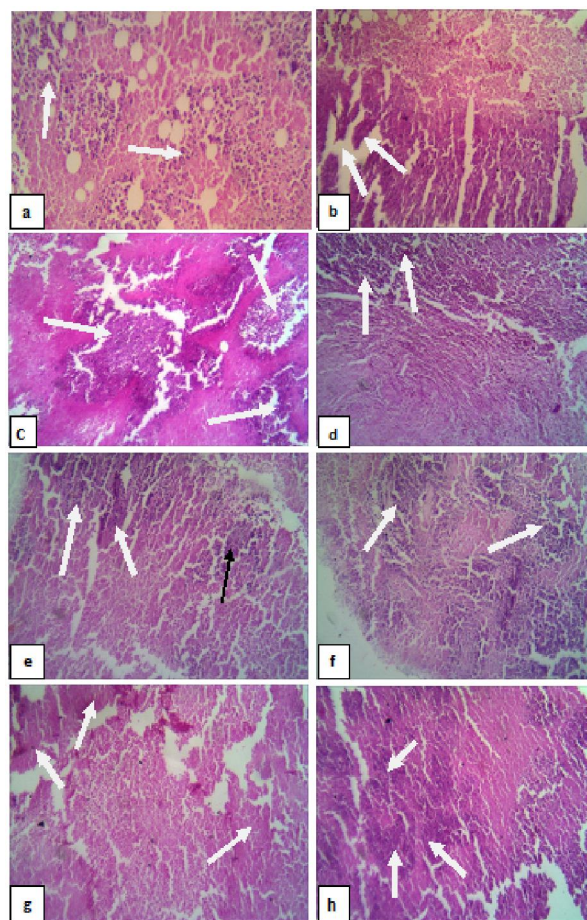
Figure 9. Histopathology of Ehrlich tumor cells with magnification x400. (A) Photomicrographs of sections in Ehrlich solid tumor (EST) stained by Hx. and E for control group (neither NPs nor MW treatment) Fig.9a: Section in Ehrlich solid tumor (EST). Fig.9b: Section in EST treated by Micro Wave. Fig.9c: Section in EST treated with Fe- NPs. Fig.9d: Section in EST treated with Fe- NPs+MW radiation. Fig.9e: Section in EST treated by treated with Ni- NPs. Fig. 9f: Section in EST treated with Ni- NPs+MW radiation. Fig.9g: Section in EST treated by treated with Co- NPs. Fig. 9h: Section in EST treated with Co- NPs+MW radiation.

Histopathological examination of the Ehrlich solid tumor (EST) under light microscope (Fig.9) with magnificationx400. Showed compact and aggregation of the tumor tissue cells spread within the muscular tissues (↑). In case of group Fig.9 (b) where tumors were treated with MW without any treatment with NPs which exhibits necrosis tumor margin. In case of sham group (Fig.9C and D) where tumors were treated with Fe-NPs and with Fe-NPs +MW respectively which exhibits tumor necrosis and fibrosis respectively. Fig.9e and f: Section in EST treated where tumors were treated with Ni-NPs and with Ni-NPs+MW respectively which exhibits tumor necrosis. Fig.9g and h: Section in EST treated where tumors were treated with Co-NPs and with Co-NPs+MW respectively which exhibits extensive necrosis.

4. Conclusions

1. We observed that nanoparticles have distinct effects on mammalian cell viability via killing cancer cells while posing no effect on normal cells. Cancer had its harmful effect on liver functions that appeared in the rising of (AST and ALT) enzymes activities. It also affected kidney functions which appeared in the rising of (Urea and Creatinine) concentrations.

2. There was highly significant decreased in the normalized tumor size with the different treatment modalities as compared with the animal bearing tumor (control group). The very high significant decreased for Ni+MW treatment was indicated i.e. the treatment of ehrlich tumor with Ni+MW give us the most inhibition for tumor.

Corresponding Author:
Dr. Sahar Ebeid Aboneima
Department of Physics, Damanhour University, Egypt.
E-mail: sahar_amr2002@yahoo.com

References

1. Franckena M and van der Zee J. Use of combined radiation and hyperthermia for gynecological cancer. Curr Opin Obstet Gynecol. 2010, 22(1):9-14.

2. Nikfarjam M, Muralidharan V, Christophi C, Mechanisms of focal heat destruction of liver tumors. J Surg Res. 2005; 127:208-223.

3. Habash RW, Bansal R, Krewski D, Alhafid HT. Thermal therapy, part 2: hyperthermia techniques. Crit Rev Biomed Eng. 2006;34 (6):491-542.

4. Rasha said Shams Eldine, M.M. Mohamed, M.B Tayel, H. Alinour, Effect of microwave hyperthermia on tumor treatment, Romanian J. Biophys.2013, 23(4), 249-259.

5. Manuel Arruebo, Rodrigo Fernández-Pacheco, M. Ricardo Ibarra, and Jesús antamaría, Magnetic nanoparticles for drug delivery.2007,2(3),22-32.

6. An-Hui Lu, E. L. Salabas, and Ferdi Schuth, Magnetic Nanoparticles: Synthesis, Protection, Functionalization, and Application, Chem. Int. Ed.2007,46,1222–1244.

7. Pushpa R Gopalan1, A.G. Annaselvi and P. Subramaniam Dr. Pushpa R Gopalan, synthesis and characterization of β-cyclodextrin capped silver nanoparticles Int. J Nanomaterials and Biostructures 2013; 3(1): 26-30.

8. Mohamed MM, Uchida T, and Minami S, Spectrosc. "A plulse - Operated Microwave-Induced plasma Source" 1989; 43: 129.

9. Masunaga, S., M. Hiraoka, M. Takahashi, S. Jo, and K. Akuta, "Clinical results of thermo radiotherapy for locally advanced and/or recurrent breast cancer-comparison of results with radiotherapy alone," Int. Journal of Hyperthermia, 1990, 6(3), 487–497.

10. Anderson, R. L., and D. S. Kapp, "Hyperthermia in cancer therapy, current status," Medical Journal Australia, 1990, 152, 310– 315.

11. Kapp, D., R. Cox, T. Barnett, and R. Ben-Yosef, "Thermo radiotherapy for residual microscopic cancer: Elective or post excisional hyperthermia and radiation therapy in the management of local-regional recurrent breast cancer," Int. Journal of Radiation Oncology Biology Physics, 1992, 24(2), 261–277.

12. Thomas, L. (1998). Alanine aminotansferase (ALT), Aspartate aminotransferase (AST), In: L.Thomas, ed., Clinical Laboratory Diagnostics, Frankfurt: TH-Books Verlagsgesellschaft, 55-65.

13. Moss, D.W., A.R. Henderson. Clinical enzymology, In: Burtis CA, Ash wood ER, eds., Tietz Textbook of Clinical Chemistry, WB Saunders Co, Philadelphia,1999, 617–721.

14. Rabab, R, Elzoghby1, Aziza Amin2, Ahlam, F, Hamouda3, and Abdel Fatah, Ali, Toxicological and pathological studies of Ivermectin on male albino rats Journal of American Science 2015; 11(3).

15. Jihyoun Lee,, Dev Kumar Chatterjee, Min Hyuk Lee, and Sunil Krishnan, Gold nanoparticles in breast cancer treatment: Promise and potential pitfalls, Cancer Lett. 2014. 28; 347(1): 46–53.

9/25/2017